

Flame region detection based on histogram backprojection

Michael Wirth and Ryan Zaremba
University of Guelph
School of Computer Science
Guelph Ontario N1G2W1 Canada
mwirth@uoguelph.ca

Abstract

Fire detection using video offers a novel way of detecting fire in spaces where conventional smoke-based fire detectors tend to exhibit high false alarm behavior. This paper explores a simple algorithm for flame detection based on the use of a modified histogram backprojection algorithm in YCbCr colour space.

1. Introduction

Fire detection is the process by which the unwanted presence of fire is detected by monitoring the environment for signs of the combustion process such as flames or smoke. In 1991 Schaenman et al [2] note that the cost of fire in Canada was around C\$11,600 million, which relates to about 2% of GDP. Similar studies in other countries have suggested the cost ranges between 0.8-2% of GDP. Methods used to detect fires can be broadly categorized into smoke, heat or radiation. They generally detect the presence of certain particles generated by smoke and flames, and issue an alarm when the particles reach the sensor. Each of these methods may be more suited to a particular environment.

Many existing detectors suffer from proximity problems, i.e. they require close proximity to the flame. In addition, they usually detect the byproducts of combustion, not always the combustion itself. Finally, they seldom provide ancillary information such as fire location, spreading rate, size, and degree of intensity. Such systems are usually extremely sensitive towards particulate matter, especially in areas such as the kitchen, where there are often many false alarms. At the other end of the spectrum are facilities such as tunnels, and warehouses, whose cavernous nature makes them challenging to protect with traditional systems. Over the past five years barn fires, and fires in large farm structures have become increasingly problematic. In 2007 there were 241 fire incidents in Ontario with an associated loss of \$57.6 million in structures. In December 2009, a fire

in ParkHill, Ontario killed 1,200 pigs and cost \$410,000 in structural losses. One of the goals of vision-based fire detection is to identify fire in such structures, where traditional fire-detection devices may be challenged. This includes (i) enclosed regions such as rail and road tunnels, (ii) atriums, warehouses and parking garages, (iii) historic buildings such as the Quebec City Armoury, and (iv) external spaces such as farms, and lumber mills.

This paper describes a simple visual flame detection algorithm based on the chromatic information extracted from a video sequence. The guiding principle of the algorithm is simplicity, as it is required to work in a device with limited computational resources.



Figure 1. An example of a well-established barn fire.

2. Vision-based fire detection

Vision-based fire detection can be defined as the process of selecting pixels within a given image, or video frame that exhibit the characteristics of fire, i.e. flame and smoke. There have been a number of attempts at vision-based fire detection systems. Healey et al. [12] explored one of the

first real-time systems for automatic fire detection using colour video input in 1993 for the purpose of detecting a burning jet fuel fire. Literature prior to this time was focused predominantly on forest fire detection, whilst there was little literature aimed at non-forest fire systems until the early 2000s. Detecting forest fire is achieved using near-static images through a difference between green (forest) and red (fire) and is therefore less algorithmically challenging. Since then a number of fire detection algorithms have been developed, some based on the colour of fire, others based on temporal characteristics, such as flame flicker [13].

Phillips et al. [14] presented a fire detection with an algorithm based on colour and temporal variations, however for fire lacking temporal differences the algorithm failed. Chen et al. [15] were the first to deal with both smoke and flame detection using a model based on colour and temporal analysis. The caveat here is that limited experimentation accompanied the work. Toreyin et al. [17] introduced a wavelet based fire detection algorithm for video. Their work is the first to form a comparison of algorithms with those of both Phillips et al. [14] and Chen et al. [15]. Their testing is extensive, using both videos containing fire, and false events. The two shortcomings are the algorithm complexity and the non-realistic nature of testing videos. Han and Lee [16] propose a fire detection system for tunnels incorporating both flame and smoke detection. They undertake extensive testing using real-fire data, but offer little in the way of quantitative results.

The most recent body of literature is that of Celik et al. [5] who propose methods of fire and smoke detection using information in the YCbCr colour space, and fuzzy logic. The work shows a high rate of detection (99%), and low false-alarm rate (4.5%), but examples are only given of forest fires. Whilst there are many new approaches to fire detection, there is no panacea for all applications. On the applications side, only in recent years have algorithms been targeted towards more divergent applications, such as expressway tunnels [18]. In the context of understanding the overall usefulness of vision-based fire detection, Gottuk et al. [19] evaluate the performance of several commercial video image detection systems in the context of shipboard fires. In 83 real-scale fire tests, the video systems detected more fires, faster than the traditional sensors.

2.1. Stages of Fire Detection

Most fire detection systems employ three major stages: (i) candidate flame pixel region identification; (ii) false-positive suppression and (iii) the analysis of flame regions. The process of fire detection is heavily reliant on the identification of appropriate flame pixels. The first stage, flame pixel identification determines the candidate regions containing pixels which may represent some part of a fire

within an image. One issue when classifying pixels as flames are false-positives, whereby pixels from non-fire objects are labeled as flames. A common means of reducing false-positive pixels is the application of flame movement detection in an image sequence. The final stage involves examining the features of fires: growth rate or size, or determine whether an alarm should be triggered.

2.2. Proposed Approach

Analyzing colour images based on colour histograms is ideal because they are rotation and scaling invariant, and immune to noise. Therefore objects can be recognized irrespective of shape. In the context of designing a real-time detection system, one of the more important aspects is that the operations involved are inherently simple, so the overall computational cost is low. Swain and Ballard [1] were the first to show how useful colour can be in identifying objects in images using the concept of *colour indexing*. Their method identifies an object in an image by comparing its colour histogram to the colour histograms of known objects stored in a database of colour histograms. An object matches a known model when its colour distribution matches those of the model. Ennesser and Medioni [3] modify the technique by localizing it to find a likely set of locations for Waldo in the *Where's Waldo* books. Yoo and Oh [4] use histogram backprojection to identify faces in tracking applications. We use histogram backprojection in YCbCr colour space in combination with a model image derived from known flame images to extract candidate flame pixel regions.

3. Flame Pixel Identification

3.1. Flame Characteristics

Flame pixels have a colouration that runs from red to orange to yellow to almost white. This scale tells you something about the energy of the fire, with the redder the flame, the less temperature and radiant heat it is releasing. Figure 2 shows a cross-section of flame profiles from a series of images containing fire. There are several distinct types of flames, *premixed* flames in which fuel vapor is mixed prior to combustion (e.g. gas stove), and *diffusion* flames in which fuel defuses into the air. This paper concerns the detection of diffusion flames.

3.2. Chromatic histograms

Colour cues may be the most important attribute when recognizing flames in fire detection. A colour space is a means of specifying colours, and they can be classified into three basic partitions [2]: HVS (human visual system)

based colour spaces (e.g. RGB), application-specific (e.g. YIQ, CMY, YCbCr), and CIE colour spaces (e.g. CIELab).

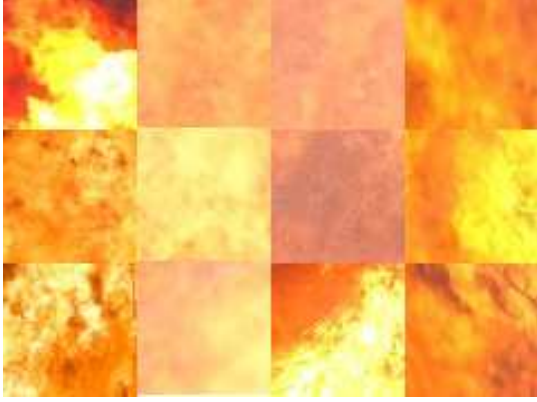


Figure 2. An example of the range of colours in flames from various fire images

Classically, colour image processing is done in RGB colour space, however RGB suffers from having the illumination information coupled with the colour channels. This basically means that if the illumination of an image changes the algorithm may no longer perform as intended. Furthermore it is impossible to decouple the intensity information from the chrominance information. Chrominance information can be used to model the colour characteristics of fire allowing for a robust representation. Several colour spaces have been proposed in the literature for flame detection including RGB [5], YUV [15], HSI [17], and YCbCr [8].

A histogram H_k represents the probability of observing a colour in the k -th bin. A 3D histogram representing RGB colour space would contain 256^3 bins, making the information too sparse to use effectively. Using a decoupled colour space such as YCbCr allows the chrominance information, represented in two channels, to be defined in a 2D histogram with only 256^2 bins. To further reduce complexity, each of the two components of the 2D histogram can be quantized into 32 levels, so there are at most 1024 bins in the 2D histogram. To create a 2D or chromatic histogram, each pixel in the input colour image is incremented in the corresponding bin. We investigate two decoupled colour spaces, YCbCr, used in video coding, and HSV due to its relevance to human colour perception.

3.3. HSV

In the HSV colour space, colours are specified by the components *hue*, *saturation* and *value*. Hue represents a pure colour as perceived by an observer. The transformation from RGB to HSV colour space is given by:

$$H = \begin{cases} 0 & \text{if } m_x = m_n \\ \frac{1}{6} \left(\frac{G-B}{m_x - m_n} \right) & \text{if } R = m_x \\ \frac{1}{6} \left(2 + \frac{B-R}{m_x - m_n} \right) & \text{if } G = m_x \\ \frac{1}{6} \left(4 + \frac{R-G}{m_x - m_n} \right) & \text{if } B = m_x \end{cases}$$

$$S = \begin{cases} 0 & \text{if } m_x = 0 \\ \frac{m_x - m_n}{m_x} & \text{otherwise} \end{cases}$$

$$V = \max(R, G, B)$$

where $m_x = \max(R, G, B)$, and $m_n = \min(R, G, B)$. All three components H, S , and V are in the range $[0, 1]$. Figure 4 shows a 3D representation of the colours in Figure 1 in HSV colour space.

3.4. YCbCr

The YCbCr colour space was developed as part of the component video standard, and belongs to the family of television transmission colour spaces. YCbCr is a scaled and offset version of the YUV colour space. Y is defined to have a nominal range of 16-235, whereas Cb and Cr have a nominal range of 16-240. Y represents the luminosity component, whilst Cb and Cr represent the chrominance of the blue (colour deviation from gray on a blue-yellow axis) and red (colour deviation from gray on a red-cyan axis) primaries respectively.

$$\begin{bmatrix} Y \\ Cb \\ Cr \end{bmatrix} = \begin{bmatrix} 0.299 & 0.587 & 0.114 \\ -0.169 & -0.331 & 0.500 \\ 0.500 & -0.419 & -0.081 \end{bmatrix} \begin{bmatrix} R \\ G \\ B \end{bmatrix}$$

Figure 4 shows a 3D representation of the colours in Figure 1 in YCbCr colour space. Figure 3 shows the components of the YCbCr representation of the image in Figure 1.

3.5. Histogram Backprojection

Histogram backprojection was introduced by Swain and Ballard [1] as a means of finding objects in a colour image by means of colour information, rather than spatial information. The basic construct is based on using histograms constructed in some colour space. By deriving histograms of both the scene of interest, or target, I , and the model image, M , the algorithm first calculates the ratio histogram of the model histogram with the scene histogram. The purpose is to create a look-up table in the particular colour space by replacing each colour appearing in the image with a value representing how closely it resembles the object to be searched



Figure 3. YCbCr components of Figure 1: Y (top), Cb (middle), Cr (bottom).

for. This histogram is then backprojected onto the image: each pixel (x,y) of colour i in the original image is replaced by its ratio value. The expected locations will appear as peaks in a smoothed version of the image.

First a model histogram M is constructed from the model image representing the object to be found, and an image histogram I is constructed from the image which is to be searched. A ratio histogram R is obtained by dividing M by I :

$$R_i = \min [M_i/I_i, 1] \quad (1)$$

where i represents the index of a bin. This ratio histogram, R is then backprojected on the image, i.e. the the image values are replaced by the values of R that they index:

$$b_{x,y} = R_{h(C_{x,y})} \quad (2)$$

where $C_{x,y}$ is the colour value at (x,y) of the input image and $h(C_{x,y})$ is the bin corresponding to $C_{x,y}$. Normally the backprojected image $b_{x,y}$ is post-processed by blur-

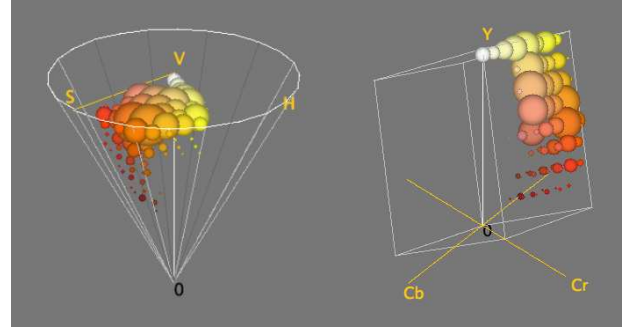


Figure 4. Fig 2 represented in HSV (left) and YCbCr (right) colour spaces.

ring, and the peak value, representing the most likely location of the model object, is identified. In this case, we use fuzzy image thresholding based on Shannon's entropy function to derive a binary representation of the most probable flame pixels [9].

4. Experimental Results

4.1. Test Data and Performance Criteria

To test the algorithm, we have chosen two sets of images. The first set contains images in which the fire is the dominant feature, from a chromaticity viewpoint. This includes images such as grass fires, forest fires and barn fires. The second set offer a more challenging environment, whereby there are non-flame features with a similar chromaticity to fire. To evaluate the performance of the algorithm, each of the images has been manually segmented to derive binary *ground truth* images. Figure 5 shows a manually extracted flame region and its corresponding binary ground truth mask. These masks are then used in conjunction with the binary images produced by the algorithms to derive the number of correctly identified flame pixels (true-positive: TP), pixels identified as flame, but which are actually not (false-positive: FP), and pixels which are flame pixels, but are not identified (false-negative: FN). To achieve this we use area-based metrics [10] to derive measures of flame detection quality: *completeness* and *correctness*. *Completeness* (CM) represents the percentage of the fire region pixels in the ground-truth which are explained by the candidate flame pixel regions detected by the algorithm. Completeness can range from 0 to 1 with 0 indicating none of the flame pixels were properly detected, and 1 indicating that all flame pixels were detected.

$$CM = \frac{TP}{TP + FN} \quad (3)$$

Correctness (CR) represents the percentage of correctly extracted candidate flame pixels in the image, from those detected. The optimum value for the correctness is 1.

$$CR = \frac{TP}{TP + FP} \quad (4)$$



Figure 5. Manually extracted flame region and binary ground truth image

4.2. Flames in Simple Scenes

The first set of images, shown in Figure 6, are simple scenes, similar to those used in testing many fire detection algorithms [5]. They consist of (clockwise from top-left): a forest fire (FF), a barn fire (BF), a brush fire (RF), and a grass fire (GF). The flames are the dominant chromatic feature, and there are very few similarly hued objects in the scenes.



Figure 6. Simple fire scenes

The backprojection algorithm was applied using both the HSV and YCbCr colour spaces in each of the images. For

Table 1. Ground-truth results for simple scenes using YCbCr backprojection

Scene	% Image flame pixels	CM	CR
Barn fire	10.16	0.71	0.98
Forest fire	26.25	0.63	0.91
Brush fire	8.6	0.89	0.55
Grass fire	3.35	0.73	0.90

example, Figure 7 shows the results of the backprojection applied to the barn scene using both HSV and YCbCr colours spaces. The HSV results appear more fragmented, due in part to the use of one chromaticity component, versus two in YCbCr. The CM and CR values for HSV are 52% and 78% respectively, indicating more false-positive pixels, and less accurate representation of the flame region. The YCbCr backprojection has produced completeness of 71%, the reduction due to redder flame regions not identified. Yet of the pixels detected, 91% represented flame pixels. The results for all simple scenes are shown in Table 1. The redder regions of flame represent the intermittent flame region with lower temperatures. Through experimentation it was determined that the HSV colour space was not as well suited to the task of flame detection.

Figure 8 shows the results for the forest fire, brush fire and grass fire using the YCbCr chromaticity components. The forest fire shows the lowest CM value, partially due to a failure in extracting the redder regions of the fire, due to their lower occurrence in the model image. The brush fire scene, has a high value of CM, but a low correctness value due to the algorithm identifying the reflection of the flame in the thermal plume as a flame region. The model image does contain similarly hued regions, so it is not unexpected. The grass fire scene has identified the major flame regions, but not the smaller, more isolated flame regions.

4.3. Flames in Complex Scenes

The second set of images, shown in Figure 9, are busy scenes which contain a multitude of similarly hued objects, and the fire is a small feature in each of the scenes. They consist of four different building fires (clockwise from top-left), labeled BF1, BF2, BF3, BF4. These scenes are used to identify potential limitations with the algorithm, as in reality such scenes, many containing advanced fires would make vision based fire detection redundant.

The complex scenes were processed using only the YCbCr colour space. Numeric results using the ground-truth images are shown in Table 2. Figure 10 shows the results for the complex fire scenes, shown top to bottom BF1 to BF4. All four images have low values for CM, due to



Figure 7. Detected flames. (clockwise) Original image, Flame-region, Backprojection-YCbCr, Backprojection-HSV

an inability to detect redder regions of fire, often on the periphery of the flames. All these images contain objects with similar hues, which is apparent in higher values of false-positive pixels detected, and lower CR values. Sources for the various FP are outlined in Table 3.

4.4. Analysis

One of the inherent difficulties with using an algorithm based on a colour model is that it is impossible to model every conceivable flame colour. In image BF4, only 38% of the flame pixels in the ground truth are detected by the BP-YCbCr algorithm. This is partially because the flame model used in the experiments (Figure 2), may not contain enough

Table 2. Ground-truth results for complex scenes using YCbCr backprojection

Scene	% Image flame pixels	CM	CR
BF1	10.38	0.55	0.78
BF2	2.00	0.46	0.61
BF3	5.15	0.62	0.69
BF4	7.38	0.38	0.46

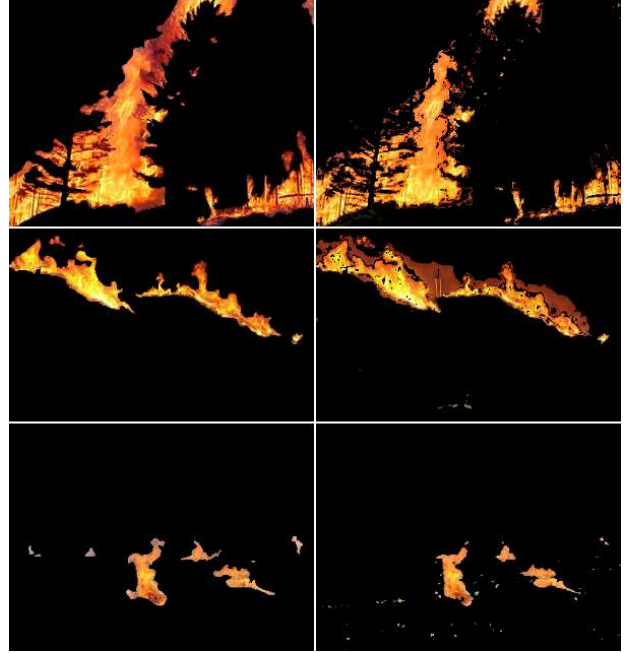


Figure 8. Results for simple fire scenes FF, RF, GF: Ground truth (left), detected flames using YCbCr backprojection (right)

Table 3. Source of false-positives in complex scenes

Scene	False positives
BF1	fire personnel uniforms, fire equipment
BF2	sun umbrella, signs
BF3	trim from truck in foreground
BF4	house siding

lower temperature (redder) fire pixels in the range necessary to characterize the flames in the image. This scene also suffers from the house having siding which has similar colour characteristics to flames, producing a CR value of 46%. If the flame model were to be changed to incorporate more reddish flames, then the result is an improved flame being detected, as shown in Figure 11. The CM and CR values increase to 0.89 and 0.64 respectively.

4.5. Multiple Flame Colours

One of the advantages of this technique is that the colour of the flame model can be easily changed, if the nature of the flame changes. For example, Figure 12 shows the burners of a natural gas furnace, whose chromaticity is blue. By using the histogram backprojection on the images using a blue-flame model, it is possible to isolate the burner



Figure 9. Complex fire scenes

flame. Such an application might be useful in determining how well the furnace burners are operating.

5. Conclusion

The purpose of this algorithm is to detect flame pixels. To that end it has produced some reasonable results, considering the complexity of some of the scenes. Whilst some of the images clearly contain false-positive objects, it is inherently difficult to derive a flame detection algorithm which is robust in all environments. There are some inherent advantages to using a chrominance based technique for finding flames. The limitations of the technique are also evident. Firstly the results are largely dependent on the choice of model used. This could be made robust by empirically determining the optimal set of colours found in the average flame pixels over a number of different fires. The algorithm used here also depends on a thresholding technique to derive a binary image, so the flame mask produced could perceptibly change if a different thresholding technique is used. However, we could also question whether detecting 100% of flames within a fire image is really necessary.

This paper has dealt with still images, identifying regions of flame pixels. Conceivably for a video-based system this step would be done for a sequence of images, using a motion-based algorithm to isolate fire regions based on flame motion. If fire is detected in a video sequence, does it really matter if only 30% of the flame region is identified? Many obvious vision-based fire detection applications would be directed, for example in a kitchen the camera would be directed towards the stove, in a utility room towards the furnace, on a farm inside a barn. This paper has outlined a simple algorithm to detect flame pixels. The experimental performed with the model used, show that this technique may be optimal in detecting flames within the *continuous* flame region [11], slightly above the base of the fire, where the fire is more constant. Future work will



Figure 10. Results for complex fire scenes: Ground truth (left), detected flames using YCbCr backprojection (right)

compare this algorithm against other chrominance based techniques to derive an optimal algorithm, and incorporate motion-based algorithms to further reduce false-positives.

References

- [1] Swain, M.J., Ballard, D.H.: Indexing via color histograms: Proc. ICCV, 390–393 (1990)
- [2] Schaenman, P., Stren, J., Bush, R.: Total cost of fire in Canada: An initial estimate. Ottawa: National Research Council of Canada (1995)
- [3] Ennesser, F., Medioni, G.: Finding Waldo or Focus of attention using local colour information: IEEE. Trans. Patt. Analysis and Mach. Intell., 17, 805–809 (1995)
- [4] Yoo, T-W., Oh, I-S.: A fast algorithm for tracking human faces based on chromatic histograms: Pattern Recognition Letters, 20, 967–978 (1999)



Figure 11. Modifying the model image, and results on image BF4

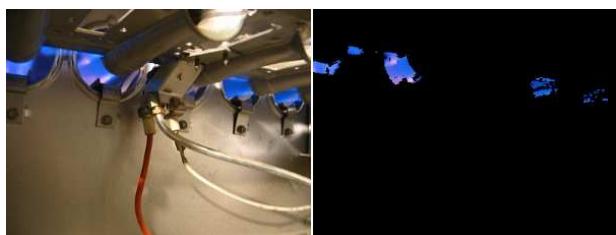


Figure 12. Detecting a natural gas flame in a series of furnace burners

- [5] Celik, T., Demirel, F.: Fire detection in video sequences using a generic color model: *Fire Safety Journal*, 44, 147-158 (2009)
- [6] Chen, T., Wu, P., Chiou, Y.: An early fire-detection method based on image processing: *IEEE Int. Conf. on Image Processing*, 1707–1710 (2004)
- [7] Toreyin, B.U., Dedeoglu, Y., Gudukbay, U., Cetin, A.E.: Computer vision based method for real-time fire and flame detection: *Pattern Recognition Letters*, 27, 49–58 (2006)
- [8] Ko, B.C., Cheong, K.H., Nam, J.Y.: Fire detection based on vision sensor and support vector machines: *Fire Safety Journal*, 44, 322–329 (2009)
- [9] Huang, L-K., Wang, M-J.J.: Image thresholding by maximizing the index of nonfuzziness of the 2-D grayscale histogram: *Pattern Recognition*, 28, 41–51 (2005)
- [10] Undrill, P., et al. Texture analysis and boundary refinement to outline mammography masses. in *EE Colloquium on Digital Mammography*. 1996. London, UK: IEE.
- [11] McCaffrey, B.J.: *Purely Buoyant Diffusion Flames: Some Experimental Results (NBSIR 79 1910)*. [U.S.] Natl. Bur. Stand., Gaithersburg, MD (1979)
- [12] Healey, G., Slater, D., Lin, T., Drda, B., Goedeke, D.A.: A system for real-time fire detection: *Computer Vision and Pattern Recognition*, 605–606 (1993)
- [13] Marbach, G., Loepfe, M., Brupbacher, T.: An image processing technique for fire detection in video images: *Fire Safety Journal*, 41, 285–289 (2006)
- [14] Phillips III, W., Shah, M., Lobo, N.: Flame recognition in video: *Pattern Recognition Letters*, 23 319–327 (2002)
- [15] Chen, T-O., Wu, P-H., Chiou, Y-C.: An early fire-detection method based on image processing: *IEEE Int. Conf., on Image Processing*, 1707–1710 (2004)
- [16] Han, D., Lee, B.: Development of early tunnel fire detection algorithm using the image processing: *Lecture Notes in Computer Science*, 4292, 39–48 (2006)
- [17] Toreyin, B.U., Dedeoglu, Y., Cetin, A.E.: Wavelet based real-time smoke detection in video: *13th European Signal Processing Conference* (2005)
- [18] Ono, T., Ishii, H., Kawamura, K., Miura, H., Momma, E., Fujisawa, T., Hozumi, J.: Application of neural network to analyses of CCD colour TV-camera image for the detection of car fires in expressway tunnels: *Fire Safety Journal*, 41, 279–284 (2006)
- [19] Gottuk, D.T., Lynch, J.A., Rose-Pehrsson, S.L., Owrutsky, J.C., Williams, F.W.: Video image fire detection for shipboard use: *Fire Safety Journal*, 41, 321–326 (2006)